Wall correction factors, P_{wall}, for thimble ionization chambers

Lesley A. Buckley[a] and D. W. O. Rogers[b]
Ottawa-Carleton Institute of Physics, Carleton University, Ottawa, K1S 5B6, Canada

(Received 15 July 2005; revised 21 October 2005; accepted for publication 23 November 2005; published 30 January 2006)

The EGSnrc Monte Carlo user-code CSnrc is used to calculate wall correction factors, P_{wall}, for thimble ionization chambers in photon and electron beams. CSnrc calculated values of P_{wall} give closer agreement with previous experimental results than do the values from the standard formalism used in current dosimetry protocols. A set of P_{wall} values, computed at the reference depth in water, is presented for several commonly used thimble chambers. These values differ from the commonly used values by up to 0.8% for megavoltage photon beams, particularly for nominal beam energies below 6 MV. The sleeve effect, which is not currently taken into account by the TG-51 dosimetry protocol, is computed to be up to 0.3% and is in some cases larger than the P_{wall} correction itself. In electron beams, where dosimetry protocols assume a wall correction of unity, CSnrc calculations show P_{wall} values of up to 0.6% at the reference depth, depending on the wall material. P_{wall} is shown to be sensitive to the depth of measurement, varying by 2.5% for a graphite-walled cylindrical Farmer-like chamber between a depth of 0.5 cm and R_{50} in a 6 MeV electron beam. [DOI: 10.1118/1.2161403]

I. INTRODUCTION

Ionization chambers are commonly used in radiation therapy to determine the absorbed dose to water in high-energy photon and electron beams. The procedure for relating the measured response of the ionization chamber to the absorbed dose to water is described by dosimetry protocols such as the AAPM's TG-51 protocol[1] and the IAEA's TRS-398 code of practice.[2] These protocols rely upon ionization chamber measurements performed in a water phantom.

The absorbed dose to water formalism employed by current dosimetry protocols uses several correction factors in transferring from the ionization chamber response to the absorbed dose to water. The correction factors must account for the presence of the chamber within the phantom since the desired quantity is the absorbed dose to a point in water, in the absence of the chamber. The ionization chamber correction factors are determined through a combination of Monte Carlo calculations, experimental measurements, and empirical formulas. Many of the correction factors used in the current dosimetry protocols are taken directly from previous, air-kerma based protocols.[3,4]

Previous studies have used Monte Carlo techniques to compute radiation dosimetry correction factors.[5–8] Such calculations are difficult since they are often in-phantom calculations and require hundreds of millions of particle histories in order to acheive reasonable statistical uncertainties in the results. The current availability of computing power and accurate Monte Carlo codes with sophisticated variance reduction techniques makes it possible to efficiently calculate a wide variety of these correction factors.

In the present study we focus upon the wall correction factor, P_{wall}, for thimble ionization chambers. The wall correction accounts for the fact that the chamber wall is composed of a material different from the phantom material. Several studies have shown that there are problems with the current values of P_{wall} used in the dosimetry protocols.[9–15]

The current calculations are performed using the EGSnrc Monte Carlo code system.[16,17] EGSnrc is the first Monte Carlo code that has been shown to simulate ion chamber response to an accuracy of 0.1%, with respect to its own cross sections.[18] The recent addition of a correlated sampling variance reduction technique to an EGSnrc user code[19] improves the calculation efficiency for ion chamber calculations.

II. THEORY

Dosimetry protocols use absorbed dose to water calibration coefficients and are based upon Spencer–Attix cavity theory. In this formulation, the dose to the water, D_{med}, is related to the dose to the cavity gas, D_{gas}, by the stopping power ratio, $(\bar{L}/\rho)^{med}_{gas}$. In an idealized case, we assume that the ion chamber does not perturb the electron spectrum, and this relationship is given by

$$D_{med} = D_{gas}\left(\frac{\bar{L}}{\rho}\right)^{med}_{gas}. \tag{1}$$

In practice, the presence of the ion chamber will affect the electron fluence spectrum and therefore corrections are required to the Spencer–Attix cavity theory. The absorbed dose to water formalism, with corrections, becomes

$$D_{med} = D_{gas}\left(\frac{\bar{L}}{\rho}\right)^{med}_{gas} P_{repl}P_{wall}P_{stem}P_{cel}. \tag{2}$$

P_{wall} accounts for the fact that the chamber wall is of a different material than the phantom. The replacement correction, P_{repl}, consists of two parts: P_{fl} and P_{gr}. P_{fl} is the fluence correction and corrects for changes in the electron fluence spectrum due to the presence of the cavity and P_{gr} is the gradient correction that accounts for the shift upstream of the effective point of measurement of the ion chamber, due to the cavity. The stem correction, P_{stem} is much smaller than

the other corrections and is often not included in the above equation. It is used to correct for the presence of the chamber stem and is included here for completeness. The central electrode correction, P_{cel}, accounts for the presence of an electrode within the cavity. For chambers that are not inherently waterproof, an additional correction factor, P_{sleeve}, is used to account for the presence of a waterproofing sleeve during the ion chamber measurements, although this can be considered to be part of P_{wall}. The sleeve correction is not included in the TG-51 formalism, however, the IAEA's TRS-398 code of practice does account for P_{sleeve}.

In electron beams, P_{wall} is traditionally assumed to be 1.00. A theoretical model developed by Nahum[20] shows the effect of the wall material on the electron spectrum in the cavity. This model shows that the wall effect in electron beams due to changes in the spectrum should be less than 1%, however there have been no systematic studies to investigate this for thimble ionization chambers.

In photon beams, dosimetry protocols use P_{wall} values given by the Almond–Svensson formula (Eq. (3)):[21]

$$P_{wall} = \frac{\alpha\left(\frac{\bar{L}}{\rho}\right)_{air}^{wall}\left(\overline{\frac{\mu_{en}}{\rho}}\right)_{wall}^{med} + (1-\alpha)\left(\frac{\bar{L}}{\rho}\right)_{air}^{med}}{\left(\frac{\bar{L}}{\rho}\right)_{air}^{med}}, \tag{3}$$

where α is the fraction of ionization in the cavity due to electrons originating in the chamber wall, $1-\alpha$ is the fraction due to electrons originating in the phantom, $(\bar{L}/\rho)_{med2}^{med1}$ is the stopping power ratio of medium 1 to medium 2, and $(\overline{\mu_{en}/\rho})_{med2}^{med1}$ is the ratio of mass-energy absorption coefficients for medium 1 to medium 2. In the limits $\alpha=0$ and $\alpha=1$, this formulation gives identical results to an alternative formula derived by Shiragai.[22,23] For physical situations, the two equations for P_{wall} give the same values, to within 0.1%.

When a waterproofing sleeve is used, the Almond–Svensson equation is extended to include the effect of the sleeve (Eq. (4)):[10,11]

$$P_{wall} = \frac{\alpha\left(\frac{\bar{L}}{\rho}\right)_{air}^{wall}\left(\overline{\frac{\mu_{en}}{\rho}}\right)_{wall}^{med} + \tau\left(\frac{\bar{L}}{\rho}\right)_{air}^{sheath}\left(\overline{\frac{\mu_{en}}{\rho}}\right)_{sheath}^{med} + (1-\alpha-\tau)\left(\frac{\bar{L}}{\rho}\right)_{air}^{med}}{\left(\frac{\bar{L}}{\rho}\right)_{air}^{med}}, \tag{4}$$

where τ is the fraction of ionization in the cavity due to electrons from the waterproofing sheath and $(1-\alpha-\tau)$ is the fraction due to electrons from the phantom.

The P_{wall} correction factor is similar to the K_{comp} correction factor used in earlier, air-kerma-based protocols.[3] In an air-kerma-based formalism, K_{comp} is used with in-air measurements to account for the composite wall materials in an ion chamber. This correction accounts for the use of a build-up cap that is not of the same material as the chamber wall. The equation for K_{comp} used by the TG-21 protocol[3] resembles the equation for P_{wall}:

$$K_{comp} = \frac{\alpha\left(\frac{\bar{L}}{\rho}\right)_{air}^{wall}\left(\overline{\frac{\mu_{en}}{\rho}}\right)_{wall}^{air} + (1-\alpha)\left(\frac{\bar{L}}{\rho}\right)_{air}^{cap}\left(\overline{\frac{\mu_{en}}{\rho}}\right)_{cap}^{air}}{\left(\frac{\bar{L}}{\rho}\right)_{air}^{wall}\left(\overline{\frac{\mu_{en}}{\rho}}\right)_{wall}^{air}}. \tag{5}$$

Here, α is the fraction of the ionization in the cavity due to electrons from the chamber wall and $(1-\alpha)$ is the fraction due to electrons that originate in the buildup cap.

As pointed out previously,[24] the above formalism for P_{wall} and K_{comp} ignores changes in attenuation. The above formulas only include the cross section data and do not include effects due to the change in density between materials. Such effects are inherently included in any experimental measurements and in Monte Carlo simulations involving materials of differing densities.

The correction factors, including P_{wall}, are used by absorbed-dose-based dosimetry protocols for determining the change with beam quality of absorbed dose calibration coefficients for ion chambers. Calibration coefficients are measured in a ^{60}Co beam and are converted to a calibration coefficient in an arbitrary beam by the factor, k_Q. In terms of the ion chamber correction factors described above and the stopping power ratios, $(\bar{L}/\rho)$, k_Q is given by

$$k_Q = \frac{\left[\left(\frac{\bar{L}}{\rho}\right)_{air}^{w} P_{wall}P_{repl}P_{cel}\right]_Q}{\left[\left(\frac{\bar{L}}{\rho}\right)_{air}^{w} P_{wall}P_{repl}P_{cel}\right]_{^{60}Co}}. \tag{6}$$

Problems with the values of the correction factors will therefore affect the value of k_Q and, in turn, will influence the calibration coefficients for the user's beam.

III. MONTE CARLO CALCULATIONS

The values of P_{wall} are computed using the EGSnrc user code, CSnrc. CSnrc uses correlated sampling as a variance

TABLE I. Details of the chamber geometries for the thimble chambers studied here. Chambers constructed from a nonconducting plastic such as PMMA have an inner graphite layer on their walls. For these chambers, both materials comprising the wall are shown, along with their thicknesses.

Chamber	Wall material	Wall thickness (g/cm^2)	Cavity length (mm)	Cavity diameter (mm)	Waterproof
A12	C-552	0.088	25.8	6.1	Y
NE2561	graphite	0.090	9.2	7.4	N
NE2571	graphite	0.061	24.0	6.4	N
NE2581	A-150	0.041	24.0	6.4	N
PR06C	C-552	0.053	22.0	6.4	N
PTW30001	PMMA	0.033	23.0	6.2	N
	+graphite	(0.012)			
PTW30004	graphite	0.079	23.0	6.2	N
Wellhöfer IC10	C-552	0.068	6.3	6.0	Y

reduction technique and can simulate a cylindrical chamber in a rectangular phantom. This user code permits multiple geometries to be simulated in a single execution of the code, maintaining correlations between similar particle trajectories within the geometries. CSnrc is based upon, and is improved from, an earlier correlated sampling code for the EGS4 Monte Carlo system.[25] The details of the correlated sampling technique as it is implemented with EGSnrc are described elsewhere.[19] For P_{wall} calculations, CSnrc improves the efficiency by a factor of 3–4 over the EGSnrc user-code CAVRZnrc.[26]

The wall correction factor, P_{wall}, corrects for the fact that the chamber wall is composed of a material different from the phantom material. Equation (2) is often applied as if the correction factors are independent and can be included in any order. However this is not, in general, true and especially for

TABLE II. Details of the input spectra used for the P_{wall} calculations. For photon beams, the nominal beam energy is shown along with the $\%dd(10)_x$ and the TPR_{10}^{20}. For electron beams, the nominal energy is shown along with R_{50} and the reference depth for each beam. The input spectra were taken from previously published works (Refs. 27–29).

Photon beams			
Description	$E_{nominal}$ (MV)	$\%dd(10)_x$[a]	TPR_{10}^{20a}
Eldorado 6 ^{60}Co	—	58.3	0.571
	4	62.7	0.616
	6	66.5	0.658
Varian Clinac	10	73.8	0.728
	15	77.7	0.750
	18	81.3	0.774
Elekta SL25	25	82.7	0.786

Electron beams			
Description	$E_{nominal}$ (MeV)	R_{50} (cm)[b]	d_{ref} (cm)
	6	2.63	1.48
	9	4.00	2.30
Varian Clinac	12	5.20	3.01
	15	6.50	3.80
	18	7.72	4.53
	6	2.18	1.21
Therac 20	9	3.42	1.95
	20	8.10	4.76
Philips SL75-20	5	2.08	1.15
Siemens KD2	21	8.30	4.88
Racetrack MM50	25	10.36	6.12

[a]Taken from Kalach and Rogers (Ref. 37).
[b]Taken from Ding and Rogers (Ref. 29).

the purposes of Monte Carlo calculations, it is important to have a consistent set of definitions for the various correction factors. In a previous CSnrc study,[19] the central electrode correction factor was computed by comparing the cavity dose for a real chamber to that for a chamber with no central electrode. The stem correction is then defined consistently by comparing the chamber with no central electrode to the same chamber with no stem. Thus, for consistency, in the current P_{wall} calculations only the air cavity, the chamber wall, and, where necessary, the waterproofing sleeve, remain. The final correction in Eq. (2) is the product $(\bar{L}/\rho)^{water}_{air} P_{repl}$, which accounts for the air cavity in the P_{wall} calculations and corrects it to a small air cavity satisfying the Spencer–Attix equation. Using these definitions of the correction factors, CSnrc is used to compute P_{wall} as the ratio of doses to the cavity for a chamber wall composed entirely of water relative to a chamber wall of the actual material and thickness used for a given chamber.

For the current P_{wall} calculations, the relevant details of the individual chamber geometries are shown in Table I. For the nonwaterproof chambers, the sleeve effect is investigated by adding a 1 mm thick PMMA waterproofing sleeve to the outside of the chamber wall in the simulation geometry. This is typical of waterproofing sleeves used in practice, although thinner PMMA sleeves are also common. CSnrc uses the same geometrical approximation used in CAVRZnrc: that is, that the cylinder is a right cylinder and does not model spherical or conical cylinder ends. For the calculations here, the cavity volume is kept the same as the air volume in the real chamber geometry.

For all of the in-phantom simulations, the ionization chamber is placed in a $30\times30\times30$ cm^3 water phantom. The midpoint of the chamber is placed at the reference depth in water, as defined by the TG-51 protocol:[1] 10 cm for photon beams, and at $d_{ref}=0.6R_{50}-0.1$ cm for electron beams, where R_{50}, expressed in centimeters, is the beam quality specifier for the electron beam. The electron cutoff energy, AE, is 521 keV and the photon cutoff energy, AP, is 10 keV. Photon splitting, with a splitting factor of 120, is used in all photon beam calculations. The incident photon spectra include a ^{60}Co spectrum[27] and several higher-energy photon spectra[28] previously published. The incident electron beam spectra are taken from the work of Ding and Rogers.[29] Table II shows the details of the input spectra. A typical in-phantom calculation in photon beams took between 20 and 30 h on each of 10 2.0 GHz machines. The CPU time for electron beam calculations varied between 3 and 14 h on the same system.

Values of P_{wall} used in the TG-51 dosimetry protocol are computed using the PROT program[30] that uses the Almond–Svensson formulation described in Eqs. (3) and (4) with a set of parameters from TG-51 for computing P_{wall}. A second, internally consistent set of P_{wall} values are computed using the Almond–Svensson formulation with all quantities computed using the EGSnrc system. The stopping-power ratios are computed using the user-code SPRRZnrc[26] and the mass energy-absorption coefficients are computed using the g user code, which is an EGSnrc user code used specifically for computing the mass energy absorption and mass energy transfer coefficients for a given medium. Values of α are computed from the TG-51 values using the PROT program and have been shown to agree reasonably well with values obtained using the EGSnrc system for the wall thicknesses used here.[31]

IV. RESULTS

A. Comparisons to measured P_{wall} and K_{comp} values in photon beams

1. Corrections for build-up caps in ^{60}Co

An experimental study by Seuntjens *et al.*[15] showed problems with the P_{wall} and K_{comp} formalism. Their measurements determined the air-kerma to absorbed-dose conversion factor:

$$C_{Co}=\frac{N^{Co}_{D,w}}{N_K}, \tag{7}$$

where $N^{Co}_{D,w}$ is the absorbed-dose-to-water calibration coefficient and N_K is the air-kerma calibration coefficient. The relation between the air-kerma and absorbed dose based calibration coefficients shows that for a given chamber, C_{Co} is inversely proportional to K_{comp}. Seuntjens *et al.* measured values of C_{Co} for a PR06C chamber with four different build-up caps. Their ratios of their measured values differed from the Almond–Svensson values by as much as 0.90%. Their experimental uncertainty on the C_{Co} values is on the order of 0.6%.

A possible source of the discrepancies between their C_{Co} values and those from the formalism is the expression for K_{comp}. If two C_{Co} values are compared for the same chamber with different buildup caps, after taking the ratio of these C_{Co} values, only the K_{comp} values remain. This provides a way to isolate the K_{comp} values for a comparison between the experiment and the K_{comp} formalism. The experimental uncertainty on C_{Co} includes both the statistical uncertainty and the uncertainty on the air kerma and absorbed dose primary standards. However, when comparing the ratio of two measured C_{Co} values, only the statistical measurement uncertainty is involved. In this case, the ratio does not depend either on the chamber specific correction factors, since the same chamber is being used, or on the systematic uncertainties due to the primary standards. Based upon the uncertainty analysis presented in Table IV of the Seuntjens *et al.* paper, the statistical uncertainty on $N_{D,w}$ is 0.08%. The statistical uncertainty on N_K is 0.09%,[32] resulting in an overall uncertainty of 0.17% on the ratio of two measured C_{Co} values.

Using the CSnrc code, it is straightforward to compute K_{comp} for a PR06C chamber in a ^{60}Co beam. Table III shows the Seuntjens *et al.* measured C_{Co} values, normalized to the C_{Co} value for the C-552 cap, for which $K_{comp}=1$, and the calculated values using standard dosimetry theory. The measured values are shown in comparison to the predictions of Eq. (5) and to the CSnrc values. The final two columns show the percent difference between the measured ratio and the ratios from CSnrc and Eq. (5), respectively. CSnrc shows

TABLE III. The ratios of the air kerma to absorbed dose calibration coefficients, C_{Co}, as measured by Seuntjens *et al.* (Ref. 15) and as computed by standard dosimetry theory, as done in TG-51 (Ref. 3). The CSnrc column shows the ratios of K_{comp} values for the different cap materials relative to a C-552 cap. The uncertainties are shown in parentheses. The uncertainties on the measured ratios are independent of the uncertainty on the standards since the ratio of values is presented. The final two columns show the percent differences between the measured values and each of the CSnrc and TG-51 values.

Cap material	Measured	CSnrc	"TG-51"	%diff. (Measured-CSnrc)	%diff. (Measured-TG-51)
C-552 (0.493 g/cm^2)	1.0	1.000	1.0	—	—
Polystyrene (0.537 g/cm^2)	0.9906(17)	0.9893(3)	0.9799	0.13%	1.08%
PMMA (0.541 g/cm^2)	0.9913(17)	0.9922(2)	0.9861	−0.09%	0.52%
Delrin (0.551 g/cm^2)	0.9942(17)	0.9934(2)	0.9902	0.08%	0.40%

much better agreement with the experimental results than do the values from the K_{comp} formalism. The largest percent difference between the CSnrc values and the measured values is 0.13%, which is within the 0.17% uncertainty, whereas this difference is as large as 1.08% ($>5\sigma$) for the values computed using the TG-51 formalism.

2. Discrepancies in values of k_Q

A study by Ross *et al.*[14] of beam quality specifiers in high-energy photon beams showed that measured ratios of the beam quality conversion factor, k_Q, did not agree with the ratio of values calculated from Eq. (6). Specifically, their measurements compared values of k_Q for an NE2571 chamber and a PR06C chamber for photon beams having $\%dd(10)_x$ in the range 82%–92%. Calculations using Eq. (6) yield a k_Q for the NE2571 chamber that is 0.4% higher than that for the PR06C chamber. Their measurements showed the reverse effect, with k_Q for the PR06C being about 0.5% greater than for the NE2571. Their estimated standard uncertainty on the ratio of k_Q values was 0.2%. Since the two chambers share the same location and cavity dimensions, the stopping power ratios and the values of P_{repl} are the same for the two chambers. This implies that the discrepancy between measured and calculated values of k_Q is caused by discrepancies in the values of P_{cel} and P_{wall} used and the real values.

Using values of P_{wall} and P_{cel} from TG-51, the calculated ratio k_Q^{NE2571}/k_Q^{PR06C} is 1.0039. As pointed out by Ross *et al.* the inclusion of the P_{cel} factor in the analysis, which was not done in their paper, worsens the agreement between the predictions of Eq. (6) and their measured ratio of 0.9950. Using CSnrc, values of P_{wall} and P_{cel} can be calculated in order to compare the ratio of k_Q values to the experimental values of Ross *et al.* These calculations were performed using the spectra from Sheikh-Bagheri and Rogers[28] and therefore needed to be slightly extrapolated in order to match the beam quality used by Ross *et al.*, having $\%dd(10)_x=84.5\%$ ($TPR_{10}^{20}=0.80$). As will be shown in a later section, P_{wall} values vary fairly smoothly in the range $\%dd(10)_x=58.9\%-82.7\%$ and therefore extrapolation is accurate. Using the current values of P_{wall} and a recent set of P_{cel} values[19] calculated using CSnrc, the ratio of k_Q for the two chambers is $0.9984\pm0.12\%$. Therefore the CSnrc values of the correction factors significantly improve the agreement between the calculated and the measured k_Q values. Table IV summarizes the values of P_{wall} and P_{cel} used in this analysis.

3. Effect of waterproofing sleeve on chamber response

The P_{wall} formalism may also be tested by investigating the effect of a waterproofing sleeve on the chamber response and comparing it to the effect predicted by Eq. (4). A study by Ross and Shortt[33] measured the effect of a waterproofing sleeve on the chamber response by varying the thickness of the sleeve. They performed measurements using an NE2571

TABLE IV. Values of the wall and central electrode correction factors used in the calculation of k_Q for the NE2571 and PR06C chambers. The correction factors are determined for a ^{60}Co beam and for a beam quality Q [$TPR_{10}^{20}=0.80$, $\%dd(10)_x=84.5$]. CSnrc values of P_{wall} are computed in the present study and P_{cel} is taken from previously published results (Ref. 19). k_Q is computed using Eq. (5) and the ratio of k_Q values for the two chambers is compared to the experimental ratio from Ross *et al.* (Ref. 14). The uncertainties in the last digit are shown in parentheses.

	Correction factor	NE2571	PR06C	k_Q^{NE2571}/k_Q^{PR06C}
CSnrc	$P_{wall}(^{60}Co)$	0.9989(7)	0.9886(7)	
	$P_{wall}(Q)$	1.0004(3)	0.9940(3)	0.9984(12)
	$P_{cel}(^{60}Co)$	0.9924(3)	1.0002(3)	
	$P_{cel}(Q)$	0.9948(3)	1.0003(3)	
TG-51	$P_{wall}(^{60}Co)$	0.9919	0.9888	
	$P_{wall}(Q)$	0.9992	0.9951	1.0039
	$P_{cel}(^{60}Co)$	0.9928	1.0000	
	$P_{cel}(Q)$	0.9957	1.0000	
Ross *et al.*	—	—	—	0.9950(20)

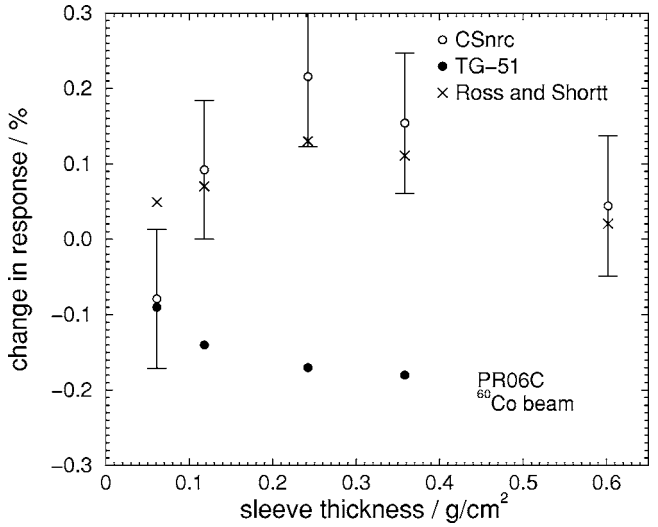

FIG. 1. The effect of a PMMA waterproofing sleeve on the response of a PR06C chamber in ^{60}Co, relative to a bare chamber. Calculated values using CSnrc are compared to measured data from Ross and Shortt and to the predictions of the TG-51 formalism. The experimental uncertainty is about 0.2% (Ref. 14).

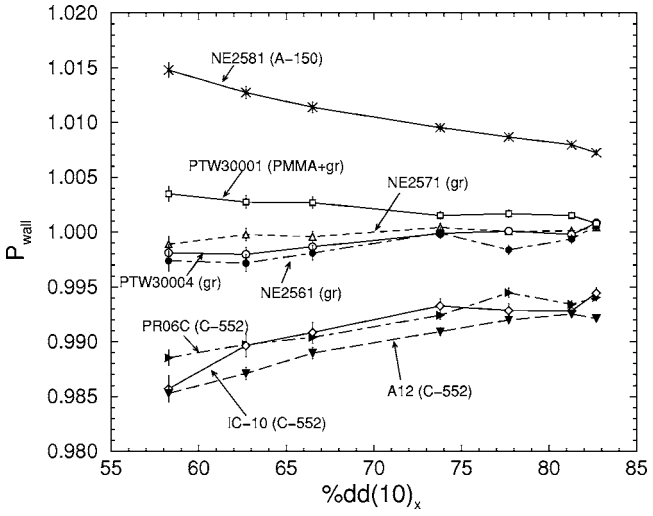

FIG. 2. P_{wall} values at a 10 cm depth for cylindrical chambers in high-energy photon beams. Shown in parentheses are the wall materials for each of the chambers. Values are calculated using CSnrc with an electron cutoff energy, AE, of 521 keV and a photon cutoff energy of 10 keV. P_{wall} values are shown for the bare chamber, without a waterproofing sleeve. Corresponding TPR^{20}_{10} values are given in Table II. The uncertainty on the CSnrc values is shown as vertical lines at each point.

and a PR06C chamber in both a ^{60}Co beam and in a 20 MV beam from the National Research Council (NRC) linear accelerator. In all cases, the chamber response was measured as a function of the material and thickness of the waterproofing sleeve. Since neither of these two chambers could be used without a waterproofing sleeve, the results were extrapolated to a sleeve thickness of 0 g/cm^2 in order to determine the effect of the sleeve relative to the bare chamber. Their results showed problems with the extended Almond–Svensson formalism of Eq. (4).

In the present study, CSnrc is used to revisit the experimental results of Ross and Shortt. The change in chamber response was calculated as a function of the material and thickness of the waterproofing sleeve and was compared to their experimental results. These calculations were performed for both an NE2571 chamber in the NRC 20 MV beam and for a PR06C chamber in a ^{60}Co beam. Both chambers were modeled with both a PMMA sleeve and a nylon sleeve. Figure 1 shows the change in the response in a ^{60}Co beam of a PR06C chamber caused by a PMMA sleeve. The measurements from Ross and Shortt agree well with the CSnrc calculations, whereas there is a significant difference between these two sets of values and the values from the Almond–Svensson formalism. In all cases, the CSnrc curves share the same shape as the experimental data and are significantly different in shape and in values from the Almond–Svensson values. For the two cases involving the nylon sleeves, there exists a discrepancy that is not completely understood (see EPAPS curves[38]). This discrepancy may be explained, at least in part, by the high variability in nylon composition, dependent on the fabrication process. There is also the possibility of a small normalization problem with the experimental results since these values had to be extrapolated to zero sleeve thickness. However, the same normalization was employed for both sleeve materials and therefore this is not likely to be a large effect since the measured PMMA results agree well with the current calculations. Despite the lack of complete agreement between the calculations and the measurements, the CSnrc and experimental curves show the same shape and agree much better than either curve does with the Almond–Svensson values.

B. Values of P_{wall} in photon beams

Since the present calculations show much better agreement with previous experimental results than does the Almond–Svensson formalism, CSnrc is used to calculate P_{wall} for a variety of commonly used ion chambers. Figure 2 shows P_{wall} values for several chambers at d_{ref} in high-energy photon beams. The P_{wall} values are shown for the chambers with no waterproofing sleeve since the TG-51 protocol ignores the effect of the waterproofing sleeve.

Current calculations of the sleeve correction using CSnrc are shown in Fig. 3 as a function of $\%dd(10)_x$. Here, P_{sleeve} is defined as the ratio of doses to the cavity for a bare chamber to that of a chamber with a waterproofing sleeve. Figure 3 shows that the presence of a 1 mm PMMA sleeve decreases the chamber response by up to 0.3% in photon beams for the chambers considered here. In some cases, this effect is larger than the P_{wall} correction itself and therefore should be included among the correction factors used by dosimetry protocols. The sleeve effect shows nearly the same behavior as a function of energy for each of the chambers and therefore the solid line in Fig. 3 includes a linear fit to the calculated sleeve effects for all the chambers as a function of the incident beam quality. The chi-squared per degree of freedom for this fit line is 1.04. Based upon the Almond–Svensson for-

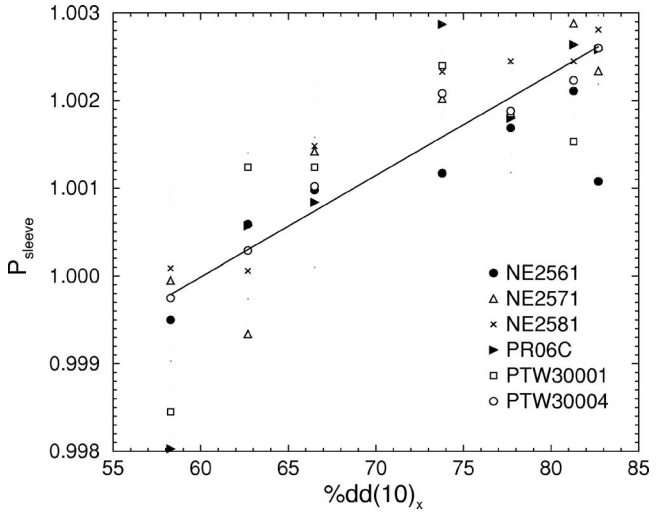

FIG. 3. The sleeve correction for a 1 mm PMMA waterproofing sleeve for a variety of cylindrical chambers in high-energy photon beams. The solid line shows a fit for all of the chambers. The statistical uncertainty on P_{sleeve} values varied from 0.1% to 0.04%. The calculations are performed using CSnrc with AE=521 keV and AP=10 keV.

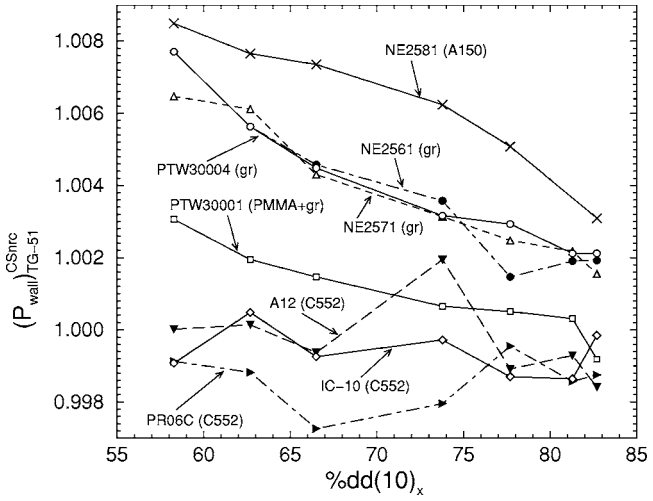

FIG. 5. The ratio of P_{wall} values as calculated using CSnrc to those predicted by the Almond–Svensson formalism with EGSnrc-calculated parameters for the cylindrical chambers studied here. The P_{wall} values are calculated for the bare chambers (with no waterproofing sleeve). The typical statistical uncertainty on the ratio is between 0.2% and 0.08%.

malism, the sleeve effect is of a similar magnitude, with P_{sleeve} varying from 0.9996 to 1.0033 over the same range of photon beam qualities.

In what follows, the CSnrc values of P_{wall} are compared to the values from the Almond–Svensson formalism (Eq. (3)) used by TG-51. For consistency, P_{wall} values are also computed using Eq. (3), where all the quantities used in this equation are computed using EGSnrc. This gives a self-consistent set of P_{wall} values, computed using the same cross-section data and calculation parameters as the CSnrc calculations. Figure 4 shows P_{wall} as a function of $\%dd(10)_x$ for an NE2571 chamber, as computed using CSnrc. Also shown are the values from the Almond–Svensson equation

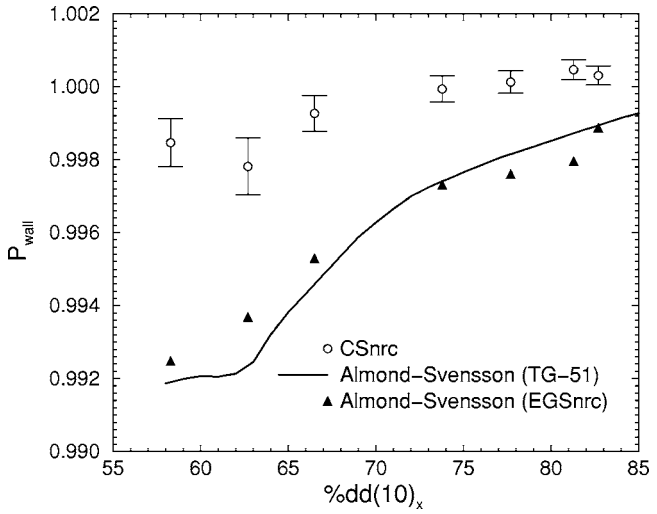

FIG. 4. P_{wall} values for an NE2571 chamber as a function of beam quality for high-energy photon beams. CSnrc calculations are compared to values from the Almond–Svensson formalism computed using the TG-51 dataset and a self-consistent set of parameters calculated using EGSnrc.

using either the TG-51 data or the self-consistent data set. For a ^{60}Co beam, there is a 0.6% difference between calculated values and the Almond–Svensson value. This plot is typical of the other graphite-walled chambers in Fig. 2, where Monte Carlo P_{wall} values differ from the predicted values by up to 0.7% for nominal energies below 6 MV. The NE2581 chamber shows differences of up to 1% at the lower energies, whereas the C-552 walled chambers agree with the theory to within 0.3% at all energies. Figure 5 shows the ratio of CSnrc values of P_{wall} to the values predicted by the Almond–Svensson formalism using the EGSnrc dataset for all of the chambers considered above.

The deviations in P_{wall} values from the formalism are slightly larger than the range of differences between measured k_Q values and the TG-51 values reported by Seuntjens *et al.*,[15] who reported an experimental uncertainty of 0.45% on their k_Q values. It is not surprising that P_{wall} shows a larger discrepancy than do the k_Q values since k_Q is only affected by the change in error in P_{wall} since it involves the ratio of P_{wall} values. For example, although the TG-51 values of P_{wall} are wrong by up to 0.8%, the new P_{wall} values imply that k_Q for graphite-walled chambers should be no more than 0.6% lower than the TG-51 values. If one looks at the measured data from Seuntjens *et al.*, the change in k_Q due to the changes in P_{wall} values still leaves good agreement between the measurements and the new k_Q values. The change in k_Q would also be affected by the sleeve correction and by any replacement corrections for a given chamber.

It is worthwhile to investigate whether differences between the present calculations and the Almond–Svensson formalism stem from the formalism itself or from the values of the parameters used in the application of the formalism. EGSnrc calculations of the parameters used in Eq. (3) show that there is no significant difference between EGSnrc values and the values used in TG-51. A comparison of EGSnrc cal-

culations of the mass energy absorption coefficient ratios, $(\mu_{en}/\rho)^{H_2O}_{med}$, show agreement with the values used in TG-51 to within 0.3% for all energies and wall materials, and in most cases, differences are less than 0.1%. EGSnrc calculations are performed using both the Storm and Israel[34] (used in EGS4/EGSnrc by default) and XCOM[35,36] photon cross-section databases. There are no significant differences between results using these two databases. Similarly, stopping-power ratios computed using the user-code SPRRZnrc, agree to within 0.1% of TG-51 values. A previous study[31] has shown that values of α used in the TG-51 protocol agree well with the EGSnrc values for the wall thicknesses considered here. Since EGSnrc values for the dosimetry parameters used in Eq. (3) are consistent with those used in TG-51, the differences between the CSnrc values of P_{wall} and the predicted values point to a problem with the Almond–Svensson formalism.

CSnrc is also well-suited to investigate the assumption used in TG-51 that P_{wall} is independent of cavity size. The CSnrc calculations are performed in both a ^{60}Co beam and in a 10 MV beam for varying cavity radii and lengths. In neither case is there any discernable (at the sub- 0.1% level) variation in P_{wall} as a function of the cavity length, however, there may be a slight dependence on the cavity radius for chamber walls showing a large P_{wall} correction (see EPAPS figures[38]).

C. P_{wall} values in electron beams

For calculations of P_{wall} for thimble chambers in high-energy electron beams, the central axis of the chamber is placed at the reference depth of $0.6R_{50}-0.1$ cm in water. Figure 6 shows P_{wall} as a function of R_{50} for the thimble chambers discussed above. The lines shown are fits to the calculated values at 11 beam qualities, ranging in nominal energy from 5 to 25 MeV. For completeness, P_{wall} is shown for beam qualities, R_{50}, between 2.08 and 10.36 cm, however, TG-51 does not recommend the use of thimble chambers for $R_{50}<4$ cm. As in the case of photon beams, P_{wall} is shown here for the bare chamber, without a waterproofing sleeve. In electron beams, the sleeve effect varies from 0.3% at $R_{50}=2.08$ cm to less than 0.1% for $R_{50}>10$ cm (see EPAPS figure). As before, this sleeve correction is in some cases greater than the P_{wall} correction itself and should not be ignored for precise work. It can be seen from Fig. 6 that for the chambers with a C-552 wall, P_{wall} is within 0.2% of unity for all electron energies. For the other chambers, P_{wall} is as high as 0.6% and is significant even for higher R_{50} values. Figure 6 also shows the P_{wall} values for the NE2571 chamber, as calculated using CSnrc. These points are typical of the scatter about the fit line for each of the chambers. In all cases, the points for the Therac input spectra ($R_{50}=2.18, 3.42, 8.10$ cm) are systematically lower than the neighboring P_{wall} values (see EPAPS figures[38]). This indicates that the value of P_{wall} is dependent on the type of beam since the Therac accelerator uses a swept beam and is nearly monoenergetic compared to the other, scattering foil machines. This suggests that R_{50} does not adequately describe the beam quality for P_{wall} investigations. When the same P_{wall} calculations are carried out using monoenergetic beams, over a similar range of R_{50} values, the value of P_{wall} decreases monotonically and shows a smooth variation as a function of R_{50}.

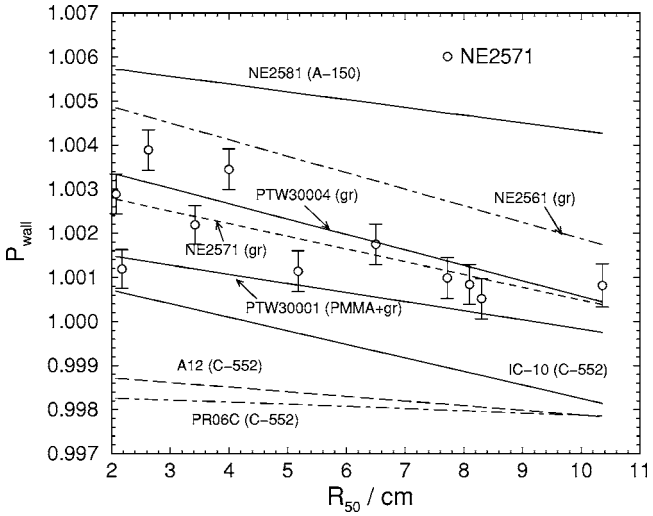

FIG. 6. Straight line fits to calculated values of P_{wall} as a function of R_{50} for thimble chambers in high-energy electron beams. Also shown are the CSnrc calculated values for the NE2571 chamber in order to show the typical scatter of points about the fit line. Calculations are performed using CSnrc with an electron cutoff energy AE=521 keV and a photon cutoff energy AP=10 keV. P_{wall} values are shown for the bare chamber, with no waterproofing sleeve and with the chamber at the reference depth, d_{ref}, in water. The TG-51 protocol and TRS-398 code of practice assume a P_{wall} of unity for all electron energies.

In electron beams, P_{wall} is very sensitive to the depth of measurement. All the above calculations were carried out at a depth of d_{ref}, as specified by the TG-51 protocol. Figure 7 shows P_{wall} as a function of the depth of measurement for an NE2571 chamber in both a 6 MeV ($R_{50}=2.63$ cm) and a 20 MeV ($R_{50}=8.10$ cm) beam. In the case of the 20 MeV

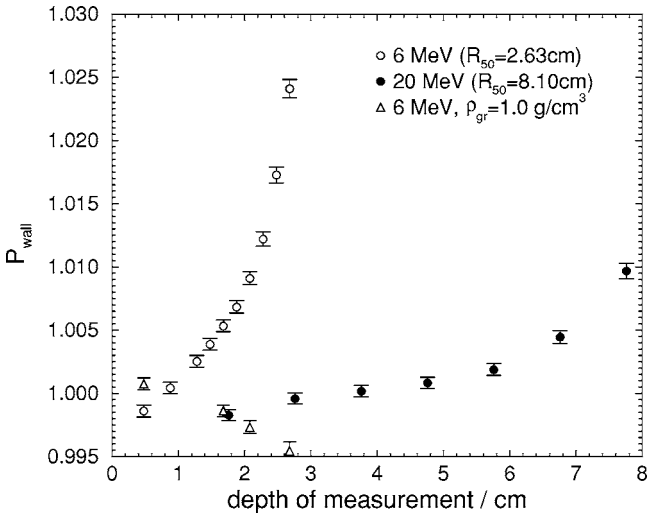

FIG. 7. P_{wall} as a function of the depth of measurement for an NE2571 chamber in a 6 MeV and a 20 MeV beam. The P_{wall} values are calculated using CSnrc with the chamber placed in a $30\times30\times30$ cm^3 water phantom.

beam, there is a 1% variation in P_{wall} when going from a depth of 2 cm to a depth of nearly R_{50}. Near d_{ref}=4.76 cm, the variation with depth is not dramatic and therefore incorrect placement of the chamber would not result in a large error in P_{wall}. In the case of the 6 MeV beam, there is a 2.5% variation in P_{wall} going from a depth of 0.5 cm to R_{50}. Near the reference depth of 1.48 cm, the gradient is steep, and therefore positioning is much more crucial for the lower-energy beam.

The variation in P_{wall} with depth can be explained in part by the difference in density between the graphite wall and the surrounding water. If the P_{wall} calculations are repeated using a graphite wall, but treating the density of the wall to be equal to that of water, the wall correction is much smaller than before and shows less variation with depth over the range of depths up to R_{50}. This is shown for the 6 MeV beam by the open triangles in Fig. 7. This suggests that the P_{wall} correction can be highly dependent on the material density. However, the material density alone cannot be used to determine P_{wall}. To investigate this possibility, if the density were the only factor influencing P_{wall}, the graphite wall in the NE2571 chamber could be considered to shift the effective depth of the chamber by 0.25 mm compared to a unit density wall. However, the relative doses at two points on the depth-dose curve separated by a depth of 0.25 mm do not correspond to P_{wall} for the real chamber at that depth, nor do we see a constant value of P_{wall} in the more or less linear part of the dose falloff region near R_{50}. The dependence on the density may indicate that the dense walls are simply stopping more electrons, an effect that increases dramatically when the average energy becomes low enough. Furthermore, while Fig. 7 shows that density has a significant effect on P_{wall}, this effect is also material dependent. Similar calculations using a PR06C chamber with C-552 walls show that the P_{wall} correction is not smaller for calculations with a unit density wall compared to the normal density case with ρ=1.76 g/cm^3.

V. CONCLUSIONS

The EGSnrc user-code CSnrc has been used to compute the wall correction factor, P_{wall}, for thimble ionization chambers. CSnrc uses a correlated sampling variance reduction technique to achieve greater calculation efficiency and yields lower statistical uncertainties than previously published values for P_{wall}. The CSnrc calculations agree better with previous experimental measurements than do the predictions of the P_{wall} formalism used in current dosimetry protocols. The CSnrc values of P_{wall} can explain the discrepancies between measured and predicted values of k_Q and between the measured and predicted effect of waterproofing sleeves and buildups caps on the chamber response. Compared to recent measurements of k_Q by Seuntjens *et al.*,[15] the new values of P_{wall} do not worsen, and in some cases improve, the agreement between the measured and predicted values.

A set of P_{wall} values has been presented for several commonly used thimble chambers in high-energy photon beams. The calculations were performed consistently, with the chamber's central axis placed at a depth of 10 cm in a 30 $\times$30$\times$30 cm^3 water phantom and no waterproofing sleeve. The sleeve effect, calculated separately and currently ignored by TG-51, was computed to be up to 0.3% and is in some cases larger than the wall correction itself. P_{wall} was shown to have no dependence on the length of the chamber cavity, although there may be a slight dependence on the radius for chamber walls with a large P_{wall} correction. When compared to the predictions of the standard P_{wall} formalism, the present set of P_{wall} values differ by up to 0.8%. A calculation of P_{wall} using the same data as in the Monte Carlo calculation and the formalism from the dosimetry protocols has shown that the problems lie with the formalism itself and not with the individual parameters used in the calculation.

For electron beams, P_{wall} values for the same set of thimble chambers have been presented, calculated at the TG-51 and TRS-398 reference depth in water. CSnrc calculations show that P_{wall} is as large as 0.6% for certain chambers, and differs from the predicted value of unity for all chambers. These calculations also show that P_{wall} is sensitive to the depth of measurement and varies by 2.5% from a depth of 0.5 cm to R_{50} in a 6 MeV beam, and that this variation is influenced greatly by the difference in density between the wall and the phantom materials.

The discrepancies between the present calculations and the currently used values in dosimetry protocols indicate the need for changes to the P_{wall} formalism now used. The new values explain many of the problems seen when comparing previous experimental measurements with the predictions of the protocols. Taking these results into account will require the reanalysis of many old experiments since many analyses have been based on incorrect values of P_{wall}. Furthermore, large P_{wall} effects in ^{60}Co beams should be considered when using thimble ionization chambers for the cross-calibration of parallel-plate chambers and in the determination of the photon-electron conversion factor, k_{ecal}. For example, for an NE2571 chamber, the 0.6% increase in P_{wall} leads to a 0.6% decrease in k_{ecal}. The nonunity values of P_{wall} in electron beams will partially offset this, but not in high-energy photon beams by more than 0.2% for the NE2571 chamber. The changes in calculated values of P_{wall} for thimble chambers also impact k_{ecal} measurements using parallel-plate chambers. Measured against an NE2571 chamber, the measured k_{ecal} values will increase by 0.6% and hence P_{wall} values will decrease by the same amount. While this trend is true of graphite-walled chambers, the C-552 walled chambers show the opposite behavior. This highlights the need to carefully take into account changes in the P_{wall} values for many dosimetry measurements.[38]

ACKNOWLEDGMENTS

The authors wish to thank their colleagues Dan La Russa, Palani Selvam, and Randle Taylor at Carleton University as well as Malcolm McEwen and Carl Ross at the National Research Council of Canada for valuable suggestions regarding this manuscript.

[a]Also at the National Research Council of Canada, Ottawa, ON K1A 0R6, Canada.
[b]Electronic mail: drogers@physics.carleton.ca

[1]P. R. Almond, P. J. Biggs, B. M. Coursey, W. F. Hanson, M. S. Huq, R. Nath, and D. W. O. Rogers, "AAPM's TG-51 protocol for clinical reference dosimetry of high-energy photon and electron beams," Med. Phys. **26**, 1847–1870 (1999).
[2]IAEA, Absorbed Dose Determination in External Beam Radiotherapy: An International Code of Practice for Dosimetry Based on Standards of Absorbed Dose to Water, Volume 398 of *Technical Report Series* (IAEA, Vienna, 2001).
[3]AAPM TG-21, "A protocol for the determination of absorbed dose from high-energy photon and electron beams," Med. Phys. **10**, 741–771 (1983).
[4]IAEA, Absorbed Dose Determination in Photon and Electron Beams; An International Code of Practice, Volume 277 of *Technical Report Series* (IAEA, Vienna, 1987).
[5]D. W. O. Rogers and A. F. Bielajew, "Wall attenuation and scatter corrections for ion chambers: measurements versus calculations," Phys. Med. Biol. **35**, 1065–1078 (1990).
[6]C.-M. Ma and A. E. Nahum, "Effect of size and composition of central electrode on the response of cylindrical ionisation chambers in high-energy photon and electron beams," Phys. Med. Biol. **38**, 267–290 (1993).
[7]C.-M. Ma and A. E. Nahum, "Dose conversion and wall correction factors for Fricke dosimetry in high-energy photon beams: analytical model and Monte Carlo calculations," Phys. Med. Biol. **38**, 93–114 (1993).
[8]C.-M. Ma and J. P. Seuntjens, "Correction factors for water-proofing sleeves in kilovoltage x-ray beams," Med. Phys. **24**, 1507–1513 (1997).
[9]A. E. Nahum, W. H. Henry, and C. K. Ross, "Response of carbon and aluminium walled thimble chamber in ^{60}Co and 20 MeV electron beams," *Proc. of VII Int. Conf. on Med. Phys, in Med. and Biol. Engin. and Comp.* 1985, Vol. 23, pp. 612–613.
[10]M. T. Gillin, R. W. Kline, A. Niroomand-Rad, and D. F. Grimm, "The effect of thickness of the waterproofing sheath on the calibration of photon and electron beams," Med. Phys. **12**, 234–236 (1985).
[11]W. F. Hanson and J. A. D. Tinoco, "Effects of plastic protective caps on the calibration of therapy beams in water," Med. Phys. **12**, 243–248 (1985).
[12]M. A. Hunt, G. J. Kutcher, and A. Buffa, "Electron backscatter correction for parallel-plate chambers," Med. Phys. **15**, 96–103 (1988).
[13]S. C. Klevenhagen, "Implications of electron backscatter for electron dosimetry," Phys. Med. Biol. **36**, 1013–1018 (1991).
[14]C. K. Ross, K. R. Shortt, D. W. O. Rogers, and F. Delaunay, "A test of TPR_{10}^{20} as a beam quality specifier for high-energy photon beams," IAEA-SM-330/10, in *Proceedings of Symposium on Measurement Assurance in Dosimetry* (IAEA, Vienna, 1994), pp. 309–321.
[15]J. P. Seuntjens, C. K. Ross, K. R. Shortt, and D. W. O. Rogers, "Absorbed-dose beam quality conversion factors for cylindrical chambers in high-energy photon beams," Med. Phys. **27**, 2763–2779 (2000).
[16]I. Kawrakow, "Accurate condensed history Monte Carlo simulation of electron transport. I. EGSnrc, the new EGS4 version," Med. Phys. **27**, 485–498 (2000).
[17]I. Kawrakow and D. W. O. Rogers, "The EGSnrc Code System: Monte Carlo simulation of electron and photon transport," Technical Report PIRS-701, National Research Council of Canada, Ottawa, Canada, 2000 (see http://www.irs.inms.nrc.ca/inms/irs/EGSnrc/EGSnrc.html).
[18]I. Kawrakow, "Accurate condensed history Monte Carlo simulation of electron transport. II. Application to ion chamber response simulations," Med. Phys. **27**, 499–513 (2000).
[19]L. A. Buckley, I. Kawrakow, and D. W. O. Rogers, "CSnrc: Correlated sampling Monte Carlo calculations using EGSnrc," Med. Phys. **31**, 3425–3435 (2004).
[20]A. E. Nahum, "Extension of the Spencer–Attix cavity theory to the 3-media situation for electron beams," in *Dosimetry in Radiotherapy* (IAEA, Vienna, 1988), Vol. 1, pp. 87–115.
[21]P. R. Almond and H. Svensson, "Ionization chamber dosimetry for photon and electron beams," Acta Radiol.: Ther., Phys., Biol. **16**, 177–186 (1977).
[22]A. Shiragai, "A proposal concerning the absorbed dose conversion factor," Phys. Med. Biol. **23**, 245–252 (1978).
[23]A. Shiragai, "Effective mass stopping power ratio in photon dosimetry," Phys. Med. Biol. **24**, 452–454 (1979).
[24]D. W. O. Rogers, "Fundamentals of high energy x-ray and electron dosimetry protocols," in *Advances in Radiation Oncology Physics, Medical Physics Monograph 19*, edited by J. Purdy (AAPM, New York, 1992), pp. 181–223.
[25]C.-M. Ma and A. E. Nahum, "Calculation of absorbed dose ratios using correlated Monte Carlo sampling," Med. Phys. **20**, 1189–1199 (1993).
[26]D. W. O. Rogers, I. Kawrakow, J. P. Seuntjens, and B. R. B. Walters, "NRC User Codes for EGSnrc," Technical Report PIRS-702, National Research Council of Canada, Ottawa, Canada, 2000.
[27]G. Mora, A. Maio, and D. W. O. Rogers, "Monte Carlo simulation of a typical ^{60}Co therapy source," Med. Phys. **26**, 2494–2502 (1999).
[28]D. Sheikh-Bagheri and D. W. O. Rogers, "Calculation of nine megavoltage photon beam spectra using the BEAM Monte Carlo code," Med. Phys. **29**, 391–402 (2002).
[29]G. X. Ding and D. W. O. Rogers, "Energy spectra, angular spread, and dose distributions of electron beams from various accelerators used in radiotherapy," National Research Council of Canada Report PIRS-0439 (see http://www.irs.inms.nrc.ca/inms/irs/papers/PIRS439/pirs439.html) (1995).
[30]D. W. O. Rogers and A. Booth, "PROT: A general purpose utility for calculating quantities related to dosimetry protocols," Technical Report PIRS-529 (rev, in preparation), NRC Canada, Ottawa, K1A 0R6.
[31]L. A. Buckley, I. Kawrakow, and D. W. O. Rogers, "An EGSnrc investigation of cavity theory for ion chambers measuring air kerma," Med. Phys. **30**, 1211–1218 (2003).
[32]P. J. Allisy-Roberts, D. T. Burns, K. R. Shortt, and C. K. Ross, "Comparison of the air kerma standards of the NRC and the BIPM for ^{60}Co γ rays," Report No. BIPM-99/12, 2000.
[33]C. K. Ross and K. R. Shortt, "The effect of waterproofing sleeves on ionization chamber response," Phys. Med. Biol. **37**, 1403–1411 (1992).
[34]E. Storm and H. I. Israel, "Photon cross sections from 1 keV to 100 MeV for elements $Z=1$ to $Z=100$," At. Data Nucl. Data Tables **7**, 565–681 (1970).
[35]M. J. Berger and J. H. Hubbell, "XCOM: Photon cross sections on a personal computer," Report No. NBSIR87-, NIST, Gaithersburg, MD 20899, 1987.
[36]J. P. Seuntjens, I. Kawrakow, J. Borg, F. Hobeila, and D. W. O. Rogers, "Calculated and measured air-kerma response of ionization chambers in low and medium energy photon beams," in *Recent Developments in Accurate Radiation Dosimetry*, Proceedings of an Int'l Workshop, edited by J. P. Seuntjens and P. Mobit (Medical Physics Publishing, Madison WI, 2002), pp. 69–84.
[37]N. I. Kalach and D. W. O. Rogers, "When is an accelerator photon beam 'clinic-like' for reference dosimetry purposes," Med. Phys. **30**, 1546–1555 (2003).
[38]See EPAPS Document No. E-MPHYA6-33-010602 for additional figures showing the wall correction factor in high energy photon and electron beams. This document can be reached via a direct link in the online article's HTML reference section or via the EPAPS homepage (http://www.aip.org/pubservs/epaps.html).